Determination of methansulfonic acid and non-sea-salt sulfate in single marine aerosol particles

ARTICLE *in* ENVIRONMENTAL SCIENCE AND TECHNOLOGY · FEBRUARY 1989

Impact Factor: 5.33 · DOI: 10.1021/es00179a018 · Source: OAI

Reprinted from ENVIRONMENTAL SCIENCE & TECHNOLOGY, Vol. 23, Page 236, February 1989

Determination of Methanesulfonic Acid and Non-Sea-Salt Sulfate in Single Marine Aerosol Particles

Leonidas N. Kolaitis, Frank J. Bruynseels, and René E. Van Grieken*

Department of Chemistry, University of Antwerp (UIA), B-2610 Antwerp-Wilrijk, Belgium

Meinrat O. Andreae

Max-Planck-Institute for Chemistry, Postbox 3060, D-6500 Mainz, West Germany

■ In open ocean waters the predominant volatile sulfur compound is dimethyl sulfide (DMS), representing almost 90% of the marine sulfur emissions. Methanesulfonic acid (MSA), one of the oxidation products of DMS, is consequently an important constituent of marine aerosols. Laser microprobe mass analysis (LAMMA) has been used for single-particle analysis of samples collected in the marine boundary layer. MSA, like the non-sea-salt sulfate, is mainly associated with the smallest aerosol particles, whose LAMMA spectra match the reference fingerprint spectra of MSA salts, sodium methanesulfonate and ammonium methanesulfonate. The presence of nitrate and heavy metal ions in the LAMMA spectra can reveal, to a certain extent, the degree of air pollution at the time of sampling.

Introduction

The volatile products of biogenic sulfate reduction such as hydrogen sulfide, carbonyl sulfide, methylmercaptan, and dimethyl sulfide (DMS) are considered to be the most important natural sources of reduced sulfur in the marine atmosphere (*1–3*). DMS is the most abundant of these compounds. Its overall flux from the world oceans is approximately 40 ± 20 Tg of S $year^{-1}$, enough to account for almost all the background non-sea-salt sulfate (nss-SO_4^{2-}) in marine aerosols (*4*).

DMS in water appears to originate from marine algae as a result of the decomposition of dimethylsulfonium propionate (DMSP), a tertiary sulfonium compound, which is present in substantial concentrations in nearly all alga species investigated (*5*). Enzymatic decomposition of DMSP produces DMS and acrylic acid in one-to-one ratio (*6*). DMS, like all volatile substances, is transferred across the air/sea interface by a combination of molecular and turbulent diffusion processes which are still poorly understood. Experimental studies (*7*) suggest that DMS in the atmosphere reacts with the hydroxyl radical, OH, during the daytime and thereby produces substantial amounts of both methanesulfonic acid (MSA) and SO_2. Preliminary experiments also indicate that MSA (CH_3SO_3H) oxidizes further to yield SO_4^{2-} (*8*). In polluted air, the nitrate radical, NO_3, exists at night in high enough concentrations to rapidly oxidize DMS (*9*, *10*), yielding as yet unknown products.

In the present study, we used the laser microprobe mass analysis (LAMMA) technique for individual particle analysis of samples collected in the marine boundary layer near the Bahamas and in the Sargasso Sea. We looked, in particular, for the MSA present in samples that were collected around noon. At this time of the day the OH concentration, and therefore also the MSA production rate, reaches its maximum value. We show that MSA is mainly concentrated in the smaller size particles (diameter d = 0.25–2 μm), as is the nss-SO_4^{2-}, suggesting gas-to-particle conversion with DMS as the gaseous precursor.

Experimental Section

Sampling. A nine-stage Battelle-type cascade impactor was used for size fractioning particle collection (*11*). It was mounted near the top of the foremast of the research vessel at ~20 m above sea level. The collection flow rate was approximately 1 L/min, the size cutoffs for stage L1, L2, 1, 2, 3, 4, 5, 6, and 7 were 0.06–0.12, 0.12–0.25, 0.25–0.5, 0.5–1, 1–2, 2–4, 4–8, 8–16, and >16 μm aerodynamic diameter, respectively. Only results for stages 1–5 will be discussed. The particles were collected on a 100-nm thick Formvar foil-backed by a copper grid. The sampling times were chosen to be 5 or 20 min, because long collection times would result in overloaded grids with particle–particle interaction interfering with the single-particle-analysis technique.

In total, three sets of samples consisting of replicate pairs of impactor stages 1–5 were analyzed. Two of them, B1 and B2, were collected in the Bahamas area during a cruise with the research vessel (R/V) Bellows (November 7–23, 1983). The third one, S1, was collected in the Sargasso Sea from the R/V Cape Hatteras (June 18–29, 1984). Many more samples were collected during both cruises for analysis with different techniques. The results of these investigations have been published elsewhere (*12*). Only the above three were collected specifically for LAMMA analysis. Sample B1 was collected on November 16, 1983, in the Southern Bahamas at 22°52′ N, 73°26′ W under tradewind and clean atmosphere conditions. B2 was collected on November 19, 1983, between Miami and Nassau, at 24°54′ N, 77°39′ W; the atmosphere was distinctly hazy with easterly winds. Sample S1 was collected on June 19, 1984, in the Sargasso Sea at 30°40′ N, 71°06′ W, in moderately polluted air with westerly winds.

Analysis. The LAMMA-500 instrument (Leybold-Heraeus, Köln, FRG), has a Nd-YAG laser (λ = 265 nm, τ = 15 ns, W = 10^{11} W/cm^2) that is focused on the sample

0013-936X/89/0923-0236$01.50/0

Table I. Bulk Composition of Samples Determined by Ion Chromatography

	sample	concn, ng m^{-3}							concn, ng of S m^{-3}		
		NH_4^+	Na	Mg	K	Ca	Cl	NO_3^-	SO_4^{2-}	nss-SO_4^{2-}	MSA
fine-fraction mode (<1.5 μm)	B1	220	55	6.2	19	4.1	17	5.1	430	425	5.3
	B2	280	130	14	11	13	70	49	730	720	5.5
	S1	315	65	17	17	28	42	15	515	510	15.7
coarse-fraction mode (>1.5 μm)	B1		3000	160	80	70	5180	600	370	120	2.1
	B2		7180	655	260	260	12260	1140	795	190	3.6
	S1	30	2250	85	85	85	2900	520	435	245	10.3
total concn	B1	220	3055	166	100	75	5195	605	800	545	7.4
	B2	280	7310	670	270	270	12330	1190	1525	910	9.0
	S1	35	2315	100	100	110	2945	535	90	755	26.0

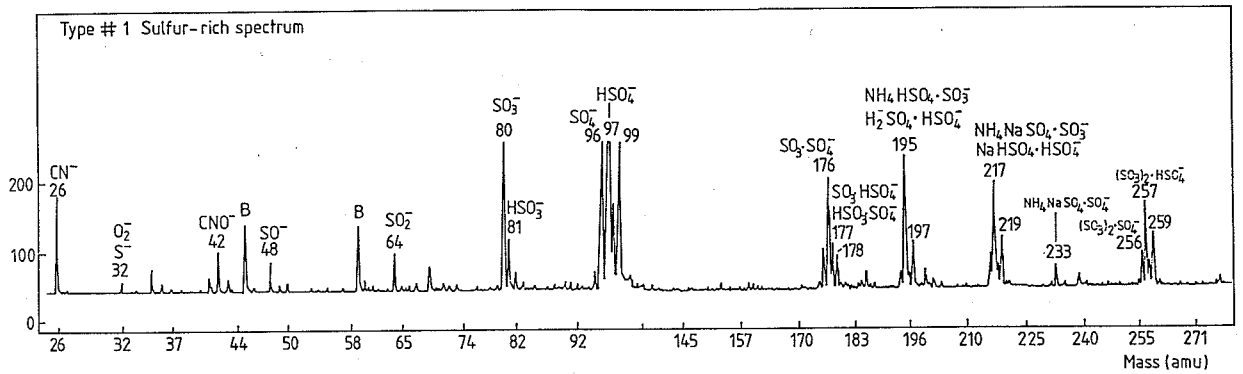

Figure 1. Sample B2; negative-mode LAMMA spectrum of type # 1. Peaks assigned with letter B are background peaks due to the Formvar.

through an optical microscope with the aid of a continuous He–Ne laser beam. The laser energy can be adjusted from 10 to 100 μJ by a 25-step optical filter system. This permits analysis of both the surface and the bulk of the particle using low or high laser energies, respectively. The produced positive (or negative) ions are focused into the time-of-flight mass spectrometer (TOF-MS) where they are mass analyzed. The LAMMA instrument is coupled via a transient recorder system with a computer. A more detailed description of the LAMMA system can be found elsewhere (*14*).

In order to avoid total destruction of the aerosol particles, low laser energies were used throughout the experiments. For each of the five stages, 100 randomly chosen particles were analyzed.

Since free methanesulfonic acid is volatile in vacuum, it cannot be detected in LAMMA, for which the samples must be introduced into an evacuated chamber. The presence of mass peaks typical for MSA in both the positive and negative ion mode suggests therefore that MSA is present in the marine aerosols as a nonvolatile salt. This was supported by the agreement of the spectra obtained from the aerosol samples with the LAMMA fingerprint spectra of sodium methanesulfonate (NaMS) and ammonium methanesulfonate (NH_4MS). Both salts proved to be nonvolatile under the vacuum in the sample chamber of the LAMMA instrument.

Results and Discussion

Sample B1 was collected just before a frontal passage carrying continental air. The atmospheric conditions were considered to be purely marine: the air was not polluted and the winds were rather weak (5 kn). DMS concentrations under such conditions are typically rather high (>100 pptv), showing a diurnal pattern due to the fluctuation of OH concentrations (*12*). Sample B2 was collected 3 days after the frontal passage, at which time the winds were rather strong and conditions classified as "continentally influenced": the atmosphere was hazy and higher nss-SO_4^{2-} concentrations indicated the presence of pollution from

Table II. Concentration of DMS [ng of S(DMS) m^{-3}] in Air for B1, B2, and S1 Samples (*12*)

collectn time	B1 16/11/1983	B2 19/11/1983	S1 19/06/1984
2:00	250	50	220
4:00	330	70	430
6:00	325	60	600
8:00	580	65	680
10:00	440	70	630
12:00	130	90	750
14:00	100	100	650
16:00	120	80	800
18:00	110	75	1000
20:00	145	60	700
22:00	110	50	690
24:00	80	45	680

North America. The presence of elevated levels of NO_x in air masses originating from the continent and the resulting nighttime formation of NO_3 caused the DMS concentration to be very low due to continuous and very fast oxidation reactions. Sample S1 was collected under strong westerly winds of 20 kn. The nns-SO_4^{2-} concentration for this sample indicated a moderately polluted air mass. Table I shows the results for MSA, nss-SO_4^{2-}, SO_4^{2-}, and other components for fine- (<1.5 μm) and coarse-mode (>1.5 μm) particles. The DMS concentrations calculated every 2 h for the same sampling periods are shown in Table II.

Analysis of Aerosol Particles from Stages 1 and 2. LAMMA spectra of the small particles in stages 1 and 2 (d = 0.25–1 μm) were indicative of sulfur-rich and carbonaceous material only. Two types of sulfur-rich spectra were observed.

A typical type # 1 spectrum, as shown in Figure 1, exhibits peaks at m/z 32, 48, 64, 80, and 96, corresponding to the SO_n^- series (n = 0–4), peaks at m/z 81 and 97 corresponding to the HSO_n^- series (n = 3, 4), as well as a peak at m/z 99 corresponding to the isotopic peak of HSO_4^- ion. This cluster ion pattern is typical for sulfur compounds such as $(NH_4)_2SO_4$ or NH_4HSO_4. In addition

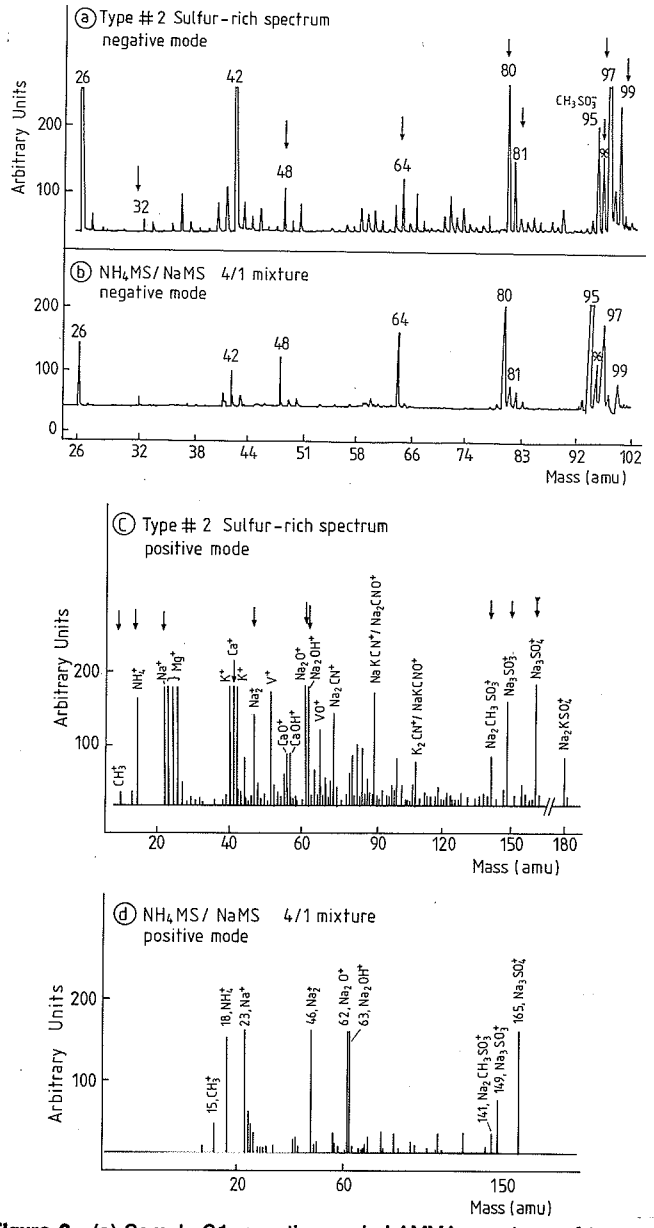

Figure 2. (a) Sample S1; negative-mode LAMMA spectrum of type # 2. (b) Negative-mode LAMMA spectrum of NH_4MS + NaMS mixture. (c) Sample S1; positive-mode LAMMA spectrum of type # 2. (d) Positive-mode LAMMA of NH_4MS + NaMS mixture. Arrows in a and c indicate that the same peaks are observed in the fingerprint spectra of NH_4MS + NaMS mixture.

to these peaks, high-mass sulfur clusters with Na^+ and/or NH_4^+ ion(s), corresponding to a mixture of sodium and ammonium sulfates, can easily be seen especially in sample B2 (Figure 1), where high nss-SO_4^{2-} compared with B1 is reported (Table I). In the corresponding positive mode, in addition to the NH_4^+ peak, Na^+ and/or K^+ clusters with sulfur were observed, being more abundant in sample B2, with peaks at m/z 143, 149, 159, 165, 181, 195, and 213 corresponding to $Na_2HSO_4^+$, $Na_3SO_3^+$, $NaKHSO_4^+$, $Na_3SO_4^+$, $Na_2KSO_4^+$, $NaK_2SO_4^+$, and $K_3SO_4^+$, respectively. The presence of all these cluster peaks and their relative intensities in both detection modes depended on the concentration of NH_4^+, Na^+, K^+ ions, which appeared to be variable among individual particles.

The other spectrum type indicative of sulfur-rich compounds (type # 2) is shown in Figure 2a,c. It shows the same sulfur pattern as in type # 1 with one additional peak; in the negative mode it appears at m/z 95 and is assigned as $CH_3SO_3^-$, while in the positive mode, it is at m/z 141 and is assigned as $Na_2CH_3SO_3^+$. The negative-mode peak was a better indicator for the presence of MSA in the particles, as the latter peak could not always be differentiated from the background noise, even when the m/z 95 peak was clearly visible.

The percentage of small particles ($d < 1$ μm) exhibiting type # 2 spectra, and thus containing MSA, was comparable for samples B1 and B2 (20–25%), whereas it was much higher for S1 (50%). Also, the relative intensity of the MSA peak at m/z 95 compared to the SO_4^- peak at m/z 96 was much higher for the S1 particles, indicating a large contribution of MSA to the sulfur in these particles. These observations were confirmed by the chromatography data of the fine-mode particles as shown in Table I; the MSA concentrations of B1 and B2 were 5.3 and 5.5 ng of S/m^3 respectively, compared to 15.7 ng of S/m^3 for S1. This was consistent with the high atmospheric DMS concentrations during the sampling period (Table II).

Analysis of Reference Samples. As mentioned above, MSA is evaporated in the vacuum of the mass spectrometer; therefore, the fingerprint spectra of its sodium and ammonium salt were used as reference spectra. The reference aerosols, with ~1-μm aerodynamic diameter, were prepared by pneumatic nebulization followed by impaction collection (*13*).

In addition to the general pattern of sulfur-containing salts, the negative spectra of both reference salts showed the $CH_3SO_3^-$ peak at m/z 95. The ammonium salt produced two more peaks assigned as $CH_3SO_3{\cdot}SO_3^-$ (m/z 175) and $CH_3SO_3{\cdot}SO_4^-$ (m/z 191), which were not found for any of the aerosol samples. This was probably due to the low concentration of MSA sulfur and/or NH_3 in the marine atmosphere. In all aerosol particles the intensity of the m/z 96 (SO_4^-) peak was higher than that of m/z 95. Their intensity ratio ranged between 7 and 70%. On the other hand, in both reference samples, the reverse was true, i.e., $CH_3SO_3^-/SO_4^-$, 2/1. Hence, the sulfur-rich particles were not wholly derived from MSA, but rather MSA partially contributed to the sulfur enrichment in these particles. The positive spectrum of NaMS contained the typical sodium sulfate peaks $Na_3SO_3^+$ (m/z 149, 40% relative intensity) and $Na_3SO_4^+$ (m/z 165, 100), as well as the $Na_2CH_3SO_3^+$ ion (m/z 141, 20). The NH_4MS generated positive peaks at m/z = 12 (C^+), m/z = 15 (CH_3^+), and m/z = 18 (NH_4^+) with relative intensities of 30, 67, and 100%, respectively. The carbon peaks were probably due to carbon bond cleavage in MSA and were also seen in a number of aerosol particles especially in association with high NH_4^+ intensities.

Once formed, MSA probably hydrates rapidly and then is incorporated into aerosols via nucleation and coagulation. MSA has a very low vapor pressure and is strongly acidic and thus is unlikely to attain an appreciable gas-phase concentration (*15*). On the other hand, MSA is quite stable in the gas phase; under atmospheric conditions it reacts only slowly with the OH radical. We propose that the MSA derivative detected in the fine-mode particles is really a mixture of its sodium and ammonium salts, since NaMS and NH_4MS are stable under vacuum and both Na^+ and NH_4^+ ions are readily available in marine aerosols. This is further supported when the negative and positive fingerprint spectra of a 4/1 mixture of NH_4MS/NaMS (Figure 2b,d) are fitted to the spectra of an MSA-containing aerosol particle (Figure 2a,c). We chose a 4/1 mixture because this approximates realistic NH_4^+/Na^+ ratios in small aerosol particles (Table I).

Analysis of Aerosol Particles from Stages 3–5. LAMMA spectra for stage 3 (d = 1–2 μm) for samples B1,

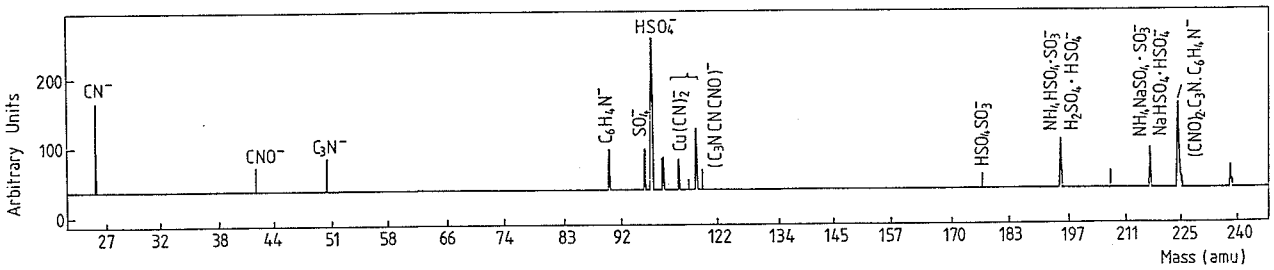

Figure 3. Sample S1; negative-mode LAMMA spectrum of amino acids and primary amines fragments.

B2, and S1 showed three different types of particles: Cl-, Cl/S-, and S-containing particles. The percentage of sulfur particles showing MSA-derived peaks was much lower in stage 3 than in 1 or 2. For B1 and B2 the Cl (sea-salt) particles were most abundant, whereas S1 contained the three types in almost equal percentages. This can also be seen in Table I, where the ratio of Cl to S concentration in the coarse mode is about 14/1 for B1 and B2 and only 7/1 for S1. On the other hand, the spectra of S- and S/Cl-containing particles in stage 3 of the S1 sample often showed MSA-derived peaks. The coarse-mode MSA concentrations in Table I confirm these findings: S1 contained 4 times more MSA than B1 and B2. For S1, it was difficult to determine the actual percentage of particles containing MSA as the m/z 95 MSA peak overlapped with the $NaCl_2^-$ peak (m/z 93, 95) in Cl/S particles. We could only detect MSA with certainty if the $NaCl_2^-$ peak did not appear, or if the intensity of the m/z 93 peak was much lower than that of the m/z 95 peak.

For stages 4 and 5 (d = 2–8 μm) of samples B1 and B2, LAMMA revealed only sea-salt particles, in agreement with earlier publications (*8*) claiming MSA to be mostly associated with the smaller particles. For sample S1, however, we still saw S and S/Cl particles that contained the MSA-derived peak, even though the percentage of sea-salt particles in these stages was clearly higher than in stage 3.

DMS, nss-SO_4^{2-}, and MSA: Correlation with Atmospheric Conditions. The stronger winds during the collection of the sample B2 compared to B1 should cause higher DMS concentrations, because of the much faster exchange rate of volatile species between the sea surface and the atmosphere. However, this was not the case; the DMS concentration for B2 was even lower than for B1 during the sampling time (Table II). This may have been due to the presence of continental air following a frontal passage, resulting in high levels of pollution-related oxidants in addition to OH, which could readily have reacted with DMS to form nss-SO_4^{2-}. On the other hand, the MSA concentration for B1 and B2 remained almost identical (Table I), which might lead to the assumption that MSA is not an end product of the DMS + NO_3 reaction.

Part of the increase of nss-SO_4^{2-} in polluted marine air was also due to advection of sulfate particles from the continent where they were mostly created by combustion processes. LAMMA spectra revealed the presence of pollution-related elements that also associate with nss-SO_4^{2-}. The moderate increase of Na^+, Mg^{2+}, and Ca^{2+} concentrations in the fine mode (Table I) in B2 compared with B1 indicates that sulfates of these elements account only partially for such a nss-SO_4^{2-} increase. Comparing samples B1 and B2 for stages 1 and 2, the near absence of Pb in B1 particles and the much less intense peaks of Ni and V were easily observed. The presence of Ni and V is a strong indicator of oil combustion, while Pb has several anthropogenic sources. All three elements were mostly concentrated in stage 1 particles. In the negative mode these particles revealed type # 1 spectra and, in very few cases, spectra containing S, Cl, and Br peaks. One possible explanation for this type of spectra is that Pb added to petrol as an antiknock agent is emitted in the atmosphere mainly as PbBrCl and Pb halides which later tend to coagulate with other particles in the air. These particles may react with sulfates and atmospheric oxidants. Ca-rich particles were observed in B2, mainly in stage 2. They may consist of various Ca compounds such as $CaSO_4$, $CaCO_3$, and CaO (*16*). $CaSO_4$ particles may be formed by differential crystallization of sea-spray droplets and subsequent breakup of the particles, or from the reaction of acid gases with $CaCO_3$.

Aluminosilicates were also present and could be divided into spherical fly-ash particles and particles of irregular shape. The former are provided by high-temperature combustion processes, while the latter can originate from low-temperature burning processes or eolian transport of mineral dust.

Other spectra exhibited mass peaks from a combination of the following elements: Al, Si, Ca, Ti, Ni, V, Mn, Fe, Cu, Ba, Pb, and NH_4^+. Because of the presence of typical "pollution" elements, the high variability in composition, and the small size, the corresponding particles were classified as pollution particles from various industrial sources.

Surface NO_3 Enrichment on Sea-Salt Particles. LAMMA desorption spectra for sample S1 in the coarse mode showed a surface nitrate enrichment of sea-salt particles that was not seen in samples B1 and B2. Table I shows that the Cl^-/NO_3^- ratio is 6/1 in S1 and 10/1 in B1 and B2; this indicates a more extensive replacement of a fraction of the sea-salt chloride by nitrate in the S1 sample. It has been shown that particulate nitrate is formed by heterogeneous reaction between HNO_3 vapor and the atmospheric particulate matter, resulting in the release of HCl from sea-salt (*13*, *17*, *18*). The first laser shot analyzing the particle surface layer revealed the presence of nitrate peaks in both the positive and negative spectrum. The peaks in the positive mode were assigned as $Na_2NO_2^+$, $NaKNO_2^+/Na_2NO_3^+$, $NaKNO_3/K_2NO_2^+$, and $K_2NO_3^+$ at m/z 92, 108, 124, and 140 respectively. In the negative mode, peaks at m/z 46, 62, 115, 131, and 147 were assigned as NO_2^-, NO_3^-, $(NaNO_3)NO^-$, $(NaNO_3)NO_2^-/(KNO_3)NO^-$, and $(NaNO_3)NO_3^-/(KNO_3)NO_2^-$. These cluster ions were matched against the $NaNO_3$ (*16*) and the KNO_3 fingerprint spectra. Subsequent laser shots revealed the presence of peaks corresponding to sea salt (Na^+ and/or K^+ with Cl^- clusters), while the intensity of the nitrate peaks was decreased with successive shots and disappeared after the third shot. The C-soot concentration for S1 was very low (13 ng/m^3), indicating that the nitrate-enriched sea-salt particles were not the result of long-range transport.

Organic Peaks in LAMMA Spectra. LAMMA also revealed spectra of particles containing only organic peaks. Dissolved free amino acids (DFAA) and primary amines are the organic fractions frequently detected in biogenic

organic matter (*19*). Their presence may have important implications in the global nitrogen cycle and may also contribute locally to available nitrogen at the sea surface. The finding of high concentrations of DFAA in rainwater and air samples (*19*) suggests that high molecular weight organic nitrogen compounds are degraded by chemical processes in the atmosphere (probably within the aerosol) to low molecular weight species, i.e., DFAA, primary amines, and ammonium. These species may also play an important role in the chemistry of atmospheric inorganic nitrogen, especially if they can be oxidized all the way to NO_3^-. If this is true, it could explain the nitrate enrichment of the sea-salt particles in sample S1. Even though these compounds also generate peaks in the LAMMA spectra, their detailed structural interpretation is not straightforward because they often overlap with the more intense peaks of the inorganic compounds.

LAMMA spectra for the small-size particles also exhibited the following peaks: in the positive mode at m/z 30 ($NH_2{=}CH_2^+$), m/z 42 ($CH_2{=}N^+{=}CH_2$), m/z 4 ($C_2H_6N^+$), and m/z 58 ($C_3H_8N^+$). In the negative mode (Figure 3), peaks at m/z 26 (CN^-), m/z 42 (CNO^-), m/z 50 (C_3N^-), m/z 74 (C_5N^-), m/z 90 ($C_6H_4N^-$), m/z 118 ($CN{\cdot}CNO{\cdot}C_3N^-$), and m/z 224 [$(CNO)_2{\cdot}C_3N{\cdot}C_6H_4N^-$] were seen. The intensities of the latter heavy clusters were always correlated to the intensities of the peaks CN^- and CNO^-. We do not claim that these high molecular weight peaks are real fragments of an amino acid or an amino-containing compound; they are produced in the plasma due to the high carbon and nitrogen concentrations in the particle.

Hydrocarbons, carboxylic acids, ketones, and alcohols were also very frequently detected in biogenic airborne organic matter. Several peaks originating from the above mentioned organic materials were reproducibly seen in the positive and negative LAMMA mode. They were assigned as follows: $(C_nH_{2n+1})^+$, n = 2–7; $(C_nH_{2n+1})^-$ n = 3; $(C_nH_{2n-1})^+$, n = 2–5; $(C_nH_{2n-1})^-$, n = 3; $(C_nH_{2n+1}O)^+$, n = 1–4; $(C_nH_{2n+1}O)^-$, n = 2, 4; $(C_nH_{2n-1}O)^-$, n = 2, 4.

Conclusions

Methanesulfonic acid (MSA) is a product of the oxidation reaction of dimethyl sulfide (DMS) by OH. The LAMMA technique was applied to aerosol samples from the Bahamas and Sargasso Sea. Individual particle analysis showed that MSA is mostly associated with the smaller particles ($d < 2$ μm) as is the nss-SO_4^{2-}. MSA itself is a volatile acid and therefore cannot be detected by LAMMA. We showed, however, that the sulfur spectra of the aerosol samples agreed with the fingerprint spectra of a mixture of ammonium- and sodium-derived MSA salt, suggesting that MDA is present as its Na^+ and NH_4^+ salt in the aerosol particles.

The Sargasso Sea sample (S1) showed an enrichment of nitrate coated on the surface of the sea-salt particles. Since the concentration of C-soot is low, it is assumed that the nitrate aerosol is not advected from the continent, but formed from the reaction of gaseous HNO_3 and sea-salt aerosol. LAMMA also revealed the presence of low molecular weight fragments of dissolved free amino acids (DFAA), primary amines, and ammonium. These species may play an important role in the chemistry of atmospheric inorganic nitrogen, especially if their end product is NO_3^-. In addition, NO_x chemistry should be very important for the fate of DMS in the marine atmosphere, but up to now the reaction products of DMS and NO_3 are still unclear.

LAMMA spectra of sample B2 also revealed the presence of pollution elements consistent with the atmospheric conditions during the sampling.

Registry No. MSA, 75-75-2; SO_4^{2-}, 14808-79-8; NH_4^+, 14798-03-9; Na, 7440-23-5; Mg, 7439-95-4; K, 7440-09-7; Ca, 7440-70-2; Cl, 7782-50-5; NO_3^-, 14797-55-8.

Literature Cited

(1) Lovelock, J. E.; Maggs, R. J.; Rasmussen, R. A. *Nature (London)* **1972**, *237*, 452.
(2) Andreae, M. O.; Raemdonck, H. *Science* **1983**, *221*, 744.
(3) Nguyen, B. G.; Bonsang, B.; Gaundry, A. *J. Geophys. Res.* **1982**, *87*, 8787.
(4) Andreae, M. O. In *The Role of Air–Sea Exchange in Geochemical Cycling*; Buat-Menard, P., Ed.; Reidel Publishing Co: Dordrecht, Holland; 1986, p 331.
(5) Ackman, R. G.; Tocher, C. S.; McLachlan, J. *J. Fish. Res. Board Can.* **1966**, *23*, 357.
(6) Challenger, F. *Aspects of the Organic Chemistry of Sulfur*; Academic Press: New York, 1959.
(7) Grosjean, D. *Environ. Sci. Technol.* **1984**, *18*, 460.
(8) Saltzman, E. S.; Savoie, D. L.; Zika, R. G.; Prospero, J. M. *J. Geophys. Res.* **1983**, *88*, 10987.
(9) Atkinson, R.; Pitts, J. N., Jr.; Aschmann, S. M. *J. Phys. Chem.* **1984**, *88*, 1584.
(10) Winer, A. M.; Atkinson, R.; Pitts, J. N., Jr. *Science* **1984**, *224*, 156.
(11) Raemdonck, H.; Maenhaut, W.; Andreae, M. O. *J. Geophys. Res.* **1986**, *91*, 8623.
(12) Andreae, M. O.; Ferek, R. J.; Bermond, F.; Byrd, K. P.; Engstrom, R. T.; Hardin, S.; Houmere, P. D.; LeMarrec, F.; Raemdonck, H.; Chatfield, R. B. *J. Geophys. Res.* **1985**, *90*, 12891.
(13) Otten, Ph.; Bruynseels, F.; Van Grieken, R. *Bull. Soc. Chim. Belg.* **1986**, *95*, 447.
(14) Vogt, H.; Heinen, H. J.; Meier, S.; Wechsung, R. *Z. Anal. Chem.* **1981**, *308*, 195.
(15) Clegg, S. L.; Brimblecombe, P. *Environ. Technol. Lett.* **1985**, *6*, 269.
(16) Bruynseels, F. Ph.D. Thesis, University of Antwerp (UIA), Belgium, 1987.
(17) Savoie, D. L.; Prospero, J. M. *Geophys. Res. Lett.* **1982**, *10*, 1207.
(18) Harrison R. M.; Pio, C. A. *Atmos. Environ.* **1983**, *17*, 1733.
(19) Mopper K.; Zika, R. G. *Nature (London)* **1987**, *325*, 246.

Received for review September 25, 1987. Accepted October 11, 1988. This work was partially supported by the Belgian Ministery of Science Policy under Grant 84-89/69 and by NATO Scientific Affairs Division under collaborative research grant 86/0812.